A Quantum Mechanical/Molecular Mechanical Approach to Relaxation Dynamics: Calculation of the Optical Properties of Solvated Bacteriochlorophyll-a

Ian P. Mercer, Ian R. Gould, and David R. Klug*

Department of Chemistry, Imperial College, South Kensington, London, SW7 2AY, U.K.

Received: January 22, 1999; In Final Form: April 28, 1999

We have applied both classical and mixed quantum mechanical/molecular mechanical (QM/MM) techniques to the calculation of electronic−vibrational coupling. In order to assess these approaches, we compare results to the steady state absorption and emission spectra of solvated bacteriochlorophyll-a (BChl-a) at room temperature. We find that the method chosen for the calculation of the S_0-S_1 energy gap significantly affects the calculated spectra. Mixed QM/MM approaches perform substantially better than the purely classical approach, and where an *ab initio* method is used for calculating the S_0-S_1 energy gap, the predicted Stokes shift (related to the reorganization energy), and the spectral absorption width are within 5% of the experimental values. We find that the decay of the transition energy correlation function occurs largely over two time scales. Most of the decorrelation occurs in less than 5 fs. This is less than the time taken for the process of photon absorption, indicating that the optical spectrum of BChl-a in methanol is predominantly homogeneous. Moreover, we find that intramolecular dynamics of the Bchl-a affect the correlation function, with a concomitant effect on the calculated observables. This is highlighted by the presence of a Franck−Condon progression in our *ab inito* calculated spectra, with the effect of this progression apparently imprinted on the corresponding free energy surface.

I. Introduction

The extent of a chemical reaction is determined by the free energy difference between reactants and products. It would be useful to be able to predict the extent, origin, and rate of development of this free energy difference in condensed phase chemical reactions. A liquid or protein will respond to a rapid change in charge distribution by structural rearrangements that minimize the energy of the system. The energy associated with these rearrangements is generally called the reorganization energy and has a well-established role in, for example, nonadiabatic electron transfer theory. The reorganization energy also appears in the response of a condensed phase chemical system to optical excitation. The creation of an excited electronic state rearranges the electron density in the molecule, leading to a rearrangement of the surrounding medium and a lowering of the excited state energy. This is revealed by the fluorescence Stokes shift which is directly related to the reorganization energy of the system.

In one sense, creation of an excited state and the subsequent Stokes shift of the fluorescence can be regarded as an extremely simple type of chemical reaction. The reactant in this case is the excited state of the molecule initially created by the applied optical field, and the product is the state created by relaxation of the system. The free energy gap between reactants and products is indicated by the shift in the peak of the steady-state absorption band from that of the steady-state emission band. The steady-state emission spectrum is a good representation of the product energy because most of the relaxation is complete well before the excited-state emits a photon. Attempts to calculate the free energy difference between initial and relaxed states in optically excited systems is a natural first step prior to calculating free energy gaps and fluctuations during more complex chemical processes. To make some progress toward this goal, we have attempted to calculate the fluorescence Stokes shift in solvated bacteriochlorophyll-a by combining classical molecular dynamics calculations with both classical and quantum mechanical calculations of the energy gap between the ground and first excited states. The shape and width of the calculated spectra are also a good indication of the ability of these calculations to reproduce the dynamics of the solvated molecule. This paper represents the first attempts at such calculations for bacteriochlorophyll-a, which has been chosen for this study because of its central role in the photosynthetic reactions of some purple bacteria.

In this work, we sample configuration space with a classical molecular dynamics simulation and calculate the electronic energy values with a classical or quantum method. In so doing we have chosen to separate the method of exploring phase space from that of evaluating each contribution of phase space to the observable. If time-ordered behavior were not required, then phase space could have been sampled in principle by a form of Monte Carlo procedure with a quantum mechanical evaluation of each element. In a similar way, our method separates the two aspects of the problem, but maintains time ordering.

Classical molecular dynamics in conjunction with classical evaluation of energy gaps has previously been applied to the calculation of optical properties of smaller solvated molecules. This yielded predictions of the shifts of the absorption and emission maxima between vacuum and solvent of indole and 3MI,[2] the Stokes shift of coumarin 153,[3] and the Stokes shift and dynamic fluorescence shift of coumarin 343.[4,5] The work which we present here is, as far as we know, the first time that a quantum mechanical evaluation of a fluctuating molecular electronic transition has been combined with a classical dynam-

* Corresponding author.

10.1021/jp990284d CCC: $18.00
Published on Web 08/21/1999

ics simulation, and the result compared with experimental data which tests the energy gap fluctuations.

Nuclear motions in the BChl-a/methanol system cause fluctuations of the electronic energy gap between ground and excited state of BChl-a. The connection between the molecular dynamics calculations and the theory required to deliver optical observables is the autocorrelation function of the time-varying electronic energy gap.[6] The autocorrelation function yields information about the system dynamics that are coupled to the electronic energy levels.

Previous classical simulations for solvated molecules suggest that after a change in electronic configuration, a significant degree of relaxation can occur in less than 200 fs.[1−5,7−17] This fast component of the system response has been assigned to inertial librational motions within the first solvation shell.[2,7] The fastest dynamics which have been obtained from classical calculations to date occur in 15 fs for 3-methylindole in water.[2] Recently, however, nonlinear optical experiments have suggested an even shorter dephasing component of 6 fs duration for solvated IR144[18] and on the order of 10 fs for solvated DTTCI.[19] It has been suggested that this extremely fast component of the dephasing is due to intramolecular dynamics. In our simulation of BChl-a in methanol, we find that the fastest component of the response is strongly dependent on the method of calculation of the energy gap. The quantum mechanical methods deliver a pronounced ultrafast component and produce an agreement with experimental data that is a substantial improvement over the classical approach. In this work, relaxation of a system to equilibrium is described by calculating the fluctuations of the system around its equilibrium position. The link between relaxation and fluctuations is established by the fluctuation dissipation theorem.[20] This requires the assumption of linear response, in which the fluctuations coupled to the system are taken to be the same for both the perturbed and equilibrium states. Linear response has been shown to hold for a wide variety of cases.[3,5,7−9]

For BChl-a solvated in methanol, we find that the method of calculating the energy gap has a significant effect on the predicted Stokes shifts, widths, and profiles of the absorption and emission spectra. Three approaches are investigated as a means to calculate the electronic energy gap: a classical method, a semiempirical quantum mechanical method, and an *ab initio* quantum mechanical method. These methods are combined with classical molecular dynamics (Newtonian mechanics) which is used to propagate the positions of nuclei.

The sampled distribution of the energy gap can be related to a free energy surface for the system.[1,21−23] In this case a Gaussian-sampled distribution for the energy gap implies that the free energy surface is quadratic and that linear response holds. In the following work, the free energy surface of the system is investigated and is found to depend on the method chosen for the determination of the energy gap. Our *ab initio* calculations agree closely with experimental data and produce a non-Gaussian distribution for the energy gap. This implies that, at least in this case, the assumption of a quadratic free energy surface, which is often assumed to hold in the condensed phase, is not valid. The appearance of a Franck−Condon progression in our spectra calculated by the *ab initio* route also serves to highlight the differences.

II. Methods

A. Obtaining Absorption and Emission Spectra from a QM/MM Simulation. The incident light field is taken to interact with two electronic levels, the ground and lowest excited singlet state of the molecule. The energy of these levels fluctuates due to interactions with the surrounding bath which results in a time-varying Bohr frequency. The time evolution of this system is described by the Liouville−von Neumann equation:[6]

$$\frac{\mathrm{d}\rho(t)}{\mathrm{d}t} = -\frac{i}{\hbar}[H(t),\rho(t)] \tag{1}$$

where $\rho(t)$ is the density operator for a two-level system with levels a and b and $H(t)$ is the Hamiltonian operator. Following an optical interaction at $t = 0$ and assuming no population loss, the solution to eq 1 is given by

$$\rho_{ab}(t) = \rho_{ab}(0)\exp(-i\omega_{ab}t)\langle\exp\{-i\int_0^t \delta\omega_{ab}(\tau)\,\mathrm{d}\tau\}\rangle \tag{2}$$

The angled brackets represents averaging over an ensemble of molecules, $\rho_{ab}(t)$ is an off-diagonal element of the density matrix, ω_{ab} is the mean angular frequency associated with the electronic energy gap, $\delta\omega_{ab}$ is the fluctuation of the energy gap from the mean value, and t is the time of the second interaction with the light field.

Finding the polarization of the ensemble requires taking the trace of the product of the transition dipole operator with the density matrix. Within the rotating wave approximation, this yields the linear optical response function, $R(t)$

$$R(t) = \langle\mu(t)\mu(0)\exp(i\int_0^t \delta\omega_{ab}(\tau)\,\mathrm{d}\tau)\rangle \tag{3}$$

Taking the distribution of fluctuations of the energy gap to be Gaussian and where sufficient phase space has been sampled, the cumulant expansion[24] can be applied to eq 3. Taking the transition dipole moment (TDM) to be constant in time (Condon approximation) and setting it to unity, the response function then becomes

$$R(t) = \exp(-g(t)) \tag{4}$$

where $g(t)$, the line-broadening function, is given by

$$g(t) = \Delta^2\int_0^t \mathrm{d}\tau_1 \int_0^{\tau_1} M(\tau_2)\,\mathrm{d}\tau_2 \tag{5}$$

and $M(t)$ is the autocorrelation function of the energy gap fluctuations scaled to unity, given by

$$M(t) = \frac{1}{\Delta^2}\int_{-\infty}^{\infty} \delta\omega_{ab}(t+\tau)\delta\omega_{ab}(\tau)\,\mathrm{d}\tau \tag{6}$$

where Δ is the root mean square deviation of the energy gap fluctuations.

Note that the ensemble average of eq 3 is now reproduced using the autocorrelation of a single variable, namely the deviation from the frequency associated with the mean energy gap (eqs 4−6). It is this frequency fluctuation which is delivered by the QM/MM simulations.

The steady state absorption and emission spectra are Fourier related to the linear response function in time (eqs 3, 4) and are given by[6,25]

$$\sigma_{ab}(\omega) \propto \mathrm{Re}[\int_0^t \mathrm{d}t\, R(t)\exp[i(\omega - \omega_{eg})t]] \tag{7a}$$

$$\sigma_{em}(\omega) \propto \mathrm{Re}[\int_0^t \mathrm{d}t\, R^*(t)\exp[i(\omega - \omega_{eg})t]] \tag{7b}$$

To find the emission spectrum, it is assumed that the excited

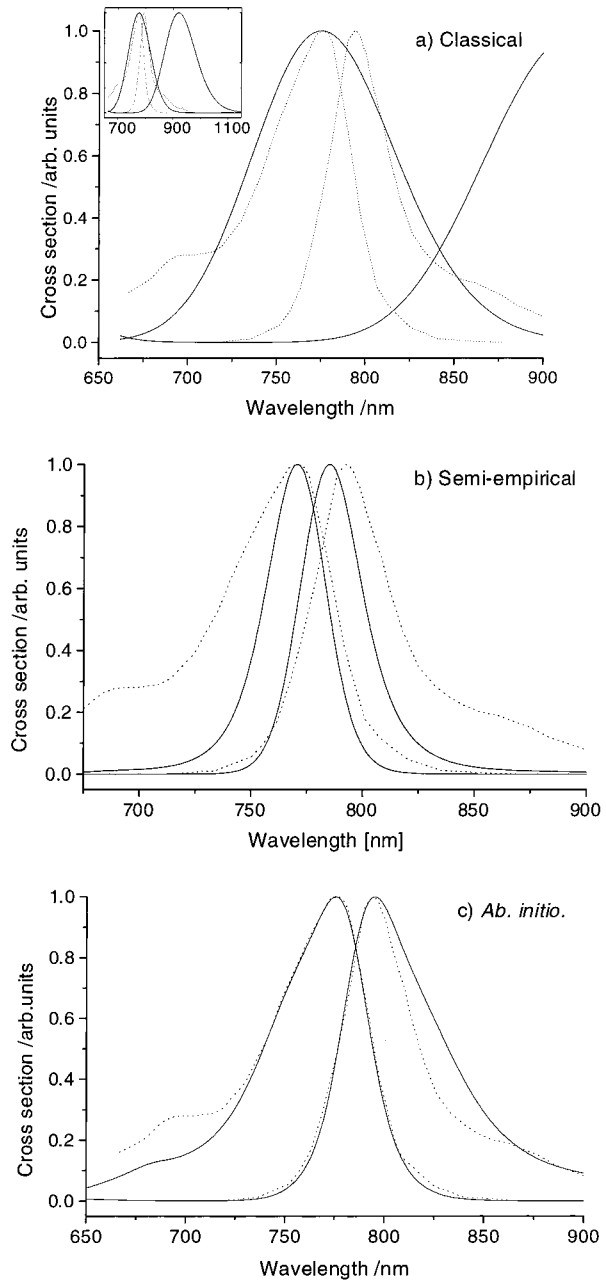

Figure 1. Optical absorption and emission spectra for BChl-a in methanol showing experimental spectra (dotted) and calculated spectra (solid) for (a) classical calculations (with full scale plot inset), (b) semiempirical quantum mechanical calculations, and (c) *ab initio* quantum mechanical calculations.

state potential energy surface has the same profile as that of the ground state, but with a minimum shifted along the relaxation coordinate. This assumption is made for convenience and to save computational cost. The fact that the profiles for the experimental absorption and emission spectra are not quite identical (see Figure 1) demonstrates that the assumption is approximate.

Up to this point, the response function $R(t)$ has been taken to be real, and as such eqs 7a and 7b are identical; there is no spectral shift between the emission and absorption spectra. In order to introduce a Stokes shift, $M(t)$ is modified to satisfy detailed balance, imparting a complex component. By asserting detailed balance, the response of the system is made to conform to the fluctuation−dissipation theorem.[20] In the context of this work, the fluctuation−dissipation theorem connects the fluctuations of an electronic energy level to its rate of relaxation following displacement from equilibrium.

Detailed balance is included by operating on the spectrum of oscillators $J(\omega)$, which is given by the Fourier transform of $M(t)$. As $M(t)$ is real and symmetric, $J(\omega)$ is necessarily also real and symmetric. However, to satisfy detailed balance it is required that positive frequencies should be related to their negative counterparts by a Boltzman coefficient,[26] such that

$$J(-\omega) = \exp(-\hbar\omega/kT)J(\omega) \tag{8}$$

To satisfy this relationship, a modified semiclassical form of the spectral density is given by[27]

$$J_{SC}(\omega) = \frac{2J(\omega)}{[1 + \exp(-\hbar\omega/kT)]} \equiv [1 + \tanh(-\hbar\omega/2kT)]J(\omega) \tag{9}$$

The semiclassical form of the spectral density is back Fourier transformed to yield a modified form of $M(t)$. Even components of a function are determined by real component in the Fourier domain, and odd components are related to complex components in the Fourier domain. With the transformation given by eq 9, the even part of the spectrum of oscillators (and hence the real part of $M(t)$) is left unchanged, and only an odd component is added, which delivers a complex part to $M(t)$. This in turn imparts a complex component for the linear response function, resulting in a Stokes shift between the calculated absorption and emission spectra (see eqs 7a,b).

Note that in the high-temperature limit, the above method yields the same result as the multimode Brownian oscillator (MBO) picture,[6] where

$$g(t) = i\lambda\int_0^t M(\tau)\,d\tau + \Delta^2\int_0^t d\tau_1\int_0^{t_1} M(\tau_2)\,d\tau_2 \tag{10}$$

and in the high-temperature limit $\lambda = \hbar\Delta^2/2kT$, where λ is the reorganization energy, Δ is the root mean squared energy gap fluctuation, k is Boltzman's constant, and T is temperature.

The time-varying transition dipole moment (TDM) (see eq 3) can also be included within the cumulant expansion approach for the calculation of the optical response. Ignoring constants in time, the linear optical response function becomes the product of three response functions, derived from the energy gap and TDM autocorrelation functions and the cross correlation between the energy gap and TDM,[28] as shown in eq 11.

$$R(t) = \exp(-g_{dd}(t) + 2i\dot{g}_{\delta d}(t) + \ddot{g}_{\delta\delta}(t)) \tag{11}$$

where g_{dd} is the line broadening function already discussed and is derived from the energy gap autocorrelation function. The other line-broadening functions, $g_{\delta\delta}$ and $g_{\delta d}$, are derived in the same manner, but substituting the energy gap autocorrelation function for the TDM autocorrelation function and the cross correlation between the energy gap and TDM, respectively. Detailed balance is asserted by adjusting the spectrum of oscillators for each individual correlation function using eq 9. We found that inclusion of the time-varying TDM has a relatively small effect on the results; however, for completeness it is included in the quantum calculations presented.

B. Quantum Mechanical/Molecular Mechanical (QM/MM) Methodology. The initial starting geometry for BChl-a was obtained from the crystal structure of Ermier et al.[29] from *R. sphaeroides*, with the phytyl chain replaced by a terminal methyl group. This resulted in a structure containing 82 atoms with the addition of hydrogen atoms as necessary to fulfill valence requirements. The hydrogen atoms (which are not seen

in the crystal structure) are added to the structures at somewhat idealized bond lengths and angles. To deal with this, the bond lengths and angles formed by these hydrogen atoms with respect to the chromophore atoms were geometry optimized to yield a low energy starting conformation, while retaining the same geometry for the non-hydrogen atoms. This was achieved using the semi-empirical quantum mechanical method due to Stewart,[30] employing the Hamiltonian known as PM3, which was performed using MOPAC-93.[31]

In order to apply the AMBER force field[32] to BChl-a, it is necessary to derive the atom-centered point charges for the ground and excited-state representations of the molecules. The AMBER force field includes standard terms for bond stretching, bond angle deformation, torsional barriers to rotation, van der Waals, and Coulombic interactions.[32]

A series of *ab initio* molecular orbital (MO) studies to investigate the ground and excited state properties of BChl-a were performed in order to determine the atom-centered point charges. Single-point configuration interaction singles (CIS) calculations (with only the core MO's frozen) were performed using Gaussian 94.[33] A hierarchical series of basis sets were used, starting with STO-3G,[34] SV 3-21G,[35] and ultimately SV 6-31G*.[36] We also investigated the use of the semiempirical PM3 Hamiltonian again using CIS to investigate the excited states of the BChl-a. Atom-centered point charges were derived for the ground and first excited states of BChl-a using the density matrices obtained with the SV 6-31G* basis set in accordance with the RESP[37] method for the AMBER force field.[32] Having developed a set of point charges for the chromophore ground and first excited state, we then performed molecular dynamics (MD) on the ground system in a bath of methanol molecules, employing the AMBER[38] suite of programs. The parameters for the methanol were provided by J. W. Caldwell[39] and these are given in Table 1. The protocol used for the MD simulations was as follows. The chromophore was placed in a cubic box of side 50 Å, containing approximately 1500 methanol molecules, resulting in a density of approximately 0.80 molecules/Å. The system was then subjected to a few hundred steps of conjugate gradient minimization[40] to alleviate any incorrect van der Waals contacts. A residue-based nonbonded cutoff of 12 Å was used for this and all subsequent simulations, where energies and forces due to the van der Waals and Coulomb interactions are neglected if the distance between all the atoms in two residues is greater than the cutoff distance. The system was then subjected to MD at constant temperature (298 K), constant pressure (1 atm), and with periodic boundary conditions. The integration time step was set to 1 fs and SHAKE[41] was applied to all stretching modes involving hydrogen atoms. Only bond stretches involving hydrogen were constrained, and no constraints were applied to bond angles or torsional barriers. The temperature control was performed by independent scaling of the velocities of the solute and solvent following the method of Berendsen.[42] An initial equilibration phase of some 80 ps was performed and equilibration was deemed to be obtained by inspection of the trace of the overall energy of the system. A data production run was then performed for 30 ps with the coordinates of the system being taken every 5 fs, resulting in a trajectory consisting of up to 6000 coordinate sets. This trajectory was then used to calculate the energy of the system for the chromophore in the excited state by replacing the charges of the chromophore ground state with those of the excited state.

We now discuss the implementation and application of the combined semiempirical quantum mechanical/molecular mechanical (QM/MM) method to BChl-a in methanol. The QM/MM method used in this study is implemented within the semiempirical package MOPAC93[31] and the *ab initio* package Gaussian 94.[33] For both the semiempirical and *ab initio* cases, the method consists of incorporating the point charges of the methanols in the one-electron Hamiltonian. This has the effect of polarizing the wave function with respect to the solvent distribution. Additionally, we could include the van der Waals interactions as well, but since these do not change in going from the ground to excited state, they have been neglected. Using the trajectories from the classical MM simulations we performed single-point calculations. The PM3 Hamiltonian was used for semiempirical calculations, and the STO-3G basis set was used for the *ab initio* calculations. The energy gap between the ground and first excited state was calculated by the CIS method in both cases. We restricted the active space available for excitation in the CIS calculations to three, five, and ten highest occupied (HOMO) and lowest unoccupied molecular orbitals (LUMO). For example, for the 3 in 3 case, the electrons in the HOMO-2, HOMO-1, and HOMO can be promoted into the LUMO, LUMO+1 and LUMO+2, and so on for the 5 in 5 and 10 in 10 cases. We performed semiempirical calculations for all three cases, but found no significant change in the derived optical observables. As such, we can assert that the choice of active orbital space is not critical for the application presented. The *ab initio* method was applied for the 10 in 10 case only.

C. Experimental Spectra. BChl-a from *R. sphaeroides* was purchased from SIGMA and used without any further purification Methanol was dried over calcium hydride and stored over

TABLE 1: Methanol AMBER Force Field Parameters[a]

atom	charge	mass	type	tree
HC1	0.0372	1.0	H1	M
C1	0.1166	12.0	CT	M
HC2	0.0372	1.0	H1	E
HC3	0.0372	1.0	H1	E
O1	−0.6497	16.0	OH	S
HO1	0.4215	1.0	HO	E

bond	K_b	R_{eq}	atom names
1	340.00	1.090	HC1−C1
2	340.00	1.090	C1−HC2
3	340.00	1.090	C1−HC3
4	553.00	0.960	O1−HO1
5	320.00	1.410	C1−O1

angle	K_θ	degrees	atom names
1	35.00	109.5	HC1−C1−HC2
2	35.00	109.5	HC1−C1−HC3
3	50.00	109.5	HC1−C1−O1
4	55.00	108.5	C1−O1−HO1
5	35.00	109.5	HC2−C1−HC3
6	50.00	109.5	HC2−C1−O1
7	50.00	109.5	HC3−C1−O1

dihedral	P_K	phase	P_N	atom names
1	0.167	0.00	3.0	HC1−C1−O1−HO1
2	0.167	0.00	3.0	HC3−C1−O1−HO1
3	0.167	0.00	3.0	HC2−C1−O1−HO1

type	R^*	EPS
CT	1.9080	0.1094
H1	1.3870	0.0157
HO	0.0000	0.0000
OH	1.7210	0.2104

[a] Bond, angle, dihedral, and nonbonded parameters used for methanol in the MD simulations. The nomenclature is the same as in Cornell et al.[32]

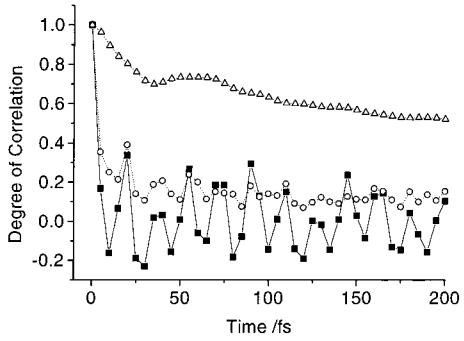

Figure 2. Energy gap correlation functions calculated with the classical (triangles), semiempirical (circles), and *ab initio* method (squares).

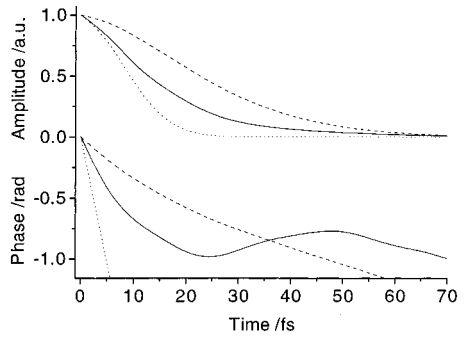

Figure 3. Linear optical response function calculated for BChl-a in methanol, using the classical (dotted), semiempirical (dashed), and *ab initio* method (solid).

a molecular sieve. The optical spectra were taken using 1 cm path length cuvettes with Bchl-a concentration of approximately 2 μM/L yielding optical densities at 774 nm of 0.1. The absorption spectrum was taken on a Perkin-Elmer Lamda2 UV−vis spectrometer while the fluorescence spectrum was measured using a SPEX Fluoromax.

III. Results

The major results are summarized by the optical absorption and emission spectra shown in Figure 1. There is substantial disagreement between calculation and experiment for the classical approach; however, the semiempirical method delivers an optical absorption width and Stokes shift to within 45% of experiment, and the *ab initio* method delivers the absorption width and Stokes shift both to within 5% of experiment. The *ab initio* method also reproduces the form of the experimental absorption profile, which includes vibrational structure via what appears to be a Franck−Condon progression.

The differences in the spectra calculated by the three methods are reflected in the correlation functions of the energy gap fluctuations, as shown in Figure 2. The derived linear optical response functions are given in Figure 3. The duration of the amplitude of the optical response function gives the electronic dephasing time, the time taken for an electronic transition to occur. As such, if the correlation function decays more quickly than the amplitude of the optical response function, then the optical profiles can be described as being largely homogeneously broadened. If, however, the correlation function decays much more slowly than the amplitude of the optical response function, the optical profiles are largely inhomogeneously broadened. From our calculations, the absorption and emission spectra for BChl-a in methanol are predicted to be inhomogeneosly broadened for the classical approach, a roughly equal mixture of homogeneous and inhomogeneous broadening for the semiempirical approach and homogeneous for the *ab initio* approach. This variation in the homogeneity of the optical spectra underlines the sensitivity of the results to the method used for the calculation of the energy gap. The *ab initio* calculations give the closest agreement with the experimental data, implying that the absorption and emission spectra are largely homogeneously broadened.

The linear optical response functions (Figure 3) also show distinct differences between the results of the three methods. The optical absorption and emission spectra are given by the real part of the Fourier transform of the linear optical response function. The gradient of the phase of the response function at $t = 0$ yields the first moment of the absorption and emission spectra relative to the energy of the mean electronic gap.

For completeness, we have included the time varying transition dipole moment (TDM) in the calculation of the optical spectra from both quantum methods (see eq 11). In the semiempirical calculations, inclusion of the time varying TDM is responsible for raising the side bands by a factor of 3, and reducing the Stokes shift by 30%. In the *ab initi*o calculations, inclusion of the time-varying TDM causes an increase in the side bands of 30% and an increase in the Stokes shift of 5%. The predicted changes are larger for the semiempirical approach mainly because the mean square deviation of the TDM is a factor of 3 larger than that for the *ab initio* approach. In neither case does the inclusion of the time-varying TDM have a significant effect on the widths of the optical profiles.

IV. Discussion

The close agreement between the calculated and experimental profiles in Figure 1c is marred by a discrepancy between the calculated and measured emission spectra. One should bear in mind, however, that all of these calculations were performed using molecular dynamics trajectories employing the ground state charge distribution of the solute. If both the excited state potential surface and the dynamics coupled to the excited state of the system were the same as that for the ground state, the experimental absorption and emission spectra would also show perfect reflective symmetry, which they do not. Given the rather close agreement between calculated and measured ground state spectra, one might expect that using the same protocol for an excited state trajectory would give good agreement for the emission spectra as well; however, we have not yet performed such calculations.

The amplitude of the vibrational structure is also not perfectly reproduced by the *ab initio* method. On the other hand, it is encouraging that such features are reproduced at all, given that the dynamics in our calculations are purely classical.

The absorption transition energy of 1.6 eV is reproduced well by the semiempirical QM method, which gives an average of 1.5 eV; however, the classical method for energy gap evaluation delivers incorrect level ordering (−0.23 eV) and the *ab initio* QM gives 2.9 eV. If one were to judge a method purely by this average static picture then one would suggest that the semiempirical method is superior to the *ab initio* calculations. In this paper, however, we are investigating method for calculating the fluctuations of a chemical system around its equilibrium position, rather than the absolute energy of the system. It is these fluctuations which lead to the difference in energy between the S_0-S_1 and S_1-S_0 transitions via the Stokes shift (see eqs 7, 8, and 9). Despite the inaccuracy of the predicted absolute transition energy for the *ab initio* method, the fluctuations of the transition energy are still well represented, as demonstrated by Figure 1c. In fact, there is no obvious correlation between the methods ability to predict the absolute transition energy and

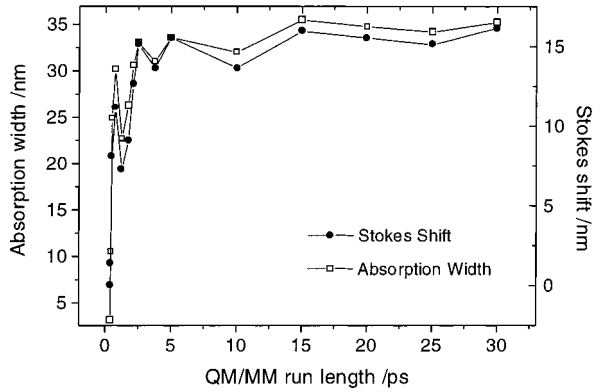

Figure 4. Stokes shift (solid circle) and absorption bandwidth (open square) vs run length for the semiempirical QM/MM calculations.

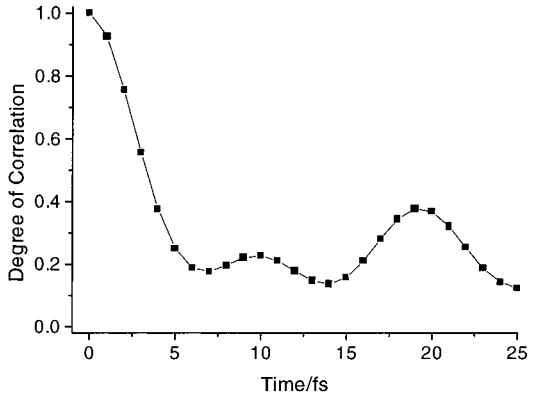

Figure 5. Autocorrelation function of the electronic energy gap $M(t)$ for BChl-a in methanol, calculated using the semiempirical method (3-HOMO, 3-LUMO) with 1 fs resolution. This shows an ultrafast component of 2−3 fs.

its ability to predict fluctuations around its equilibrium position. To reflect this, the calculated absorption and emission spectra have been shifted in energy by the same amount so that the peaks of the calculated and experimental absorption spectra coincide. By these means, each method's ability to predict the extent of relaxation becomes apparent by comparing experimental and calculated Stokes shift.

It is at first sight rather surprising that the three methods presented for calculating the energy gap produce such different dynamic responses, particularly when the same nuclear trajectory (calculated by classical MD techniques) is used in all three cases. The differences are clearly displayed in the correlation functions (Figure 2). In essence the coupling of nuclear dynamics to the electronic transition energy differs for the three approaches. In other words, the three methods of calculation sample differently the strength of electron−vibration coupling for the various modes of the system.

In order to accurately reproduce the observed properties of the molecular ensemble, it is necessary to sample an adequate portion of the phase space of the chemical system under consideration. We estimated the length of trajectory required for good sampling using the semiempirical method. In Figure 4, the Stokes shift and absorption width converge at the same rate with the values having largely stabilized with an MD run duration of approximately 2.2 ps. Beyond this duration of run, neither optical observable changes significantly. Closer investigation reveals that the rate of convergence is limited by the requirement to sample vibrations with a period of approximately 2.2 ps, corresponding to a frequency of 15 cm^{-1}. It is for this reason that a run length of 2.5 ps was chosen for the much more expensive *ab initio* calculations. The good agreement between calculation and measurement in Figure 1c suggests that we have indeed sampled an appropriate portion of phase space in 2.5 ps.

The autocorrelation function of the *ab initio* energy gap is dominated by a fast (<5 fs) decaying component and an 18 fs oscillatory component with an amplitude of 0.4. The absorption and emission spectra can be strongly affected by dynamics associated with the fastest fluctuations, with the 18 fs component manifested as a sideband within the main spectral profile (see Figure 1c). The semiempirical method yields similar components for the autocorrelation function, but in this case the oscillatory component has an amplitude of only 0.12 peak to peak, and the autocorrelation function includes a prominent 2.2 ps component with an amplitude of 0.1 peak to peak.

One of the more surprising findings in these calculations is the extreme rapidity of the decay of the autocorrelation function for both methods that involve a quantum calculation of the energy gap (see Figure 2). Figure 2 shows the correlation function for the semiempirical calculations over the first 200 fs. The autocorrelation function drops to roughly half its initial value in 2−3 fs. The rapidity of this drop might lead one to worry that the 5 fs gaps between evaluations of the energy gap might not be sampling the early time correlation function well. To check this, we used the computationally cheaper semiempirical method with a 1 fs evaluation step. The optical spectra produced were indistinguishable from those produced with the 5 fs evaluation step length, but the rapidity of the memory loss is illustrated in Figure 5 using the 1 fs step data. At these early times, the autocorrelation function is nominally Gaussian as opposed to being purely exponential. This ultrafast component is necessary to successfully reproduce the experimental spectra, suggesting that it is genuine.

There have been suggestions that the line-shape functions for solvated molecules are dominated by solvent motion. However, recent nonlinear wave-mixing experiments on solvated molecules have yielded components of electronic dephasing on a 10 fs time scale.[18,19] Such components are faster than those expected from dynamics associated with the first solvation shell and they have been attributed instead to intramolecular dynamics of the solute. We find that vibrational modes over a broad range of frequencies contribute to the very fast dynamics, and we suspect that many of these modes are intramolecular. Indeed, the rapidity and the intramolecular nature of the 2−3 fs component may explain why we have been able to reproduce experimental data accurately without taking into account solvent polarizability.

It is sometimes helpful to express the energy gap fluctuations as a collective coordinate. This is most readily done by plotting the probability of a given transition energy (plotted on a logarithmic scale) versus the energy gap value, as shown in Figure 6. A Gaussian probability distribution for the fluctuations will produce a quadratic solvation energy surface. Although this is the case for the classical calculations, and to some extent for the semiempirical results, the fluctuations for the *ab initio* calculations are far from Gaussian, yielding in turn a solvation energy surface which deviates from a parabolic profile even for energies as low as k_BT.

It is worth noting that a non-Gaussian distribution of values for a microscopic variable (in this case the transition energy) does not violate the central limit theorem. The central limit theorem can only be applied to deliver a Gaussian distribution of means when, along with other constraints one is sampling to find each mean value over a number of coupled modes that

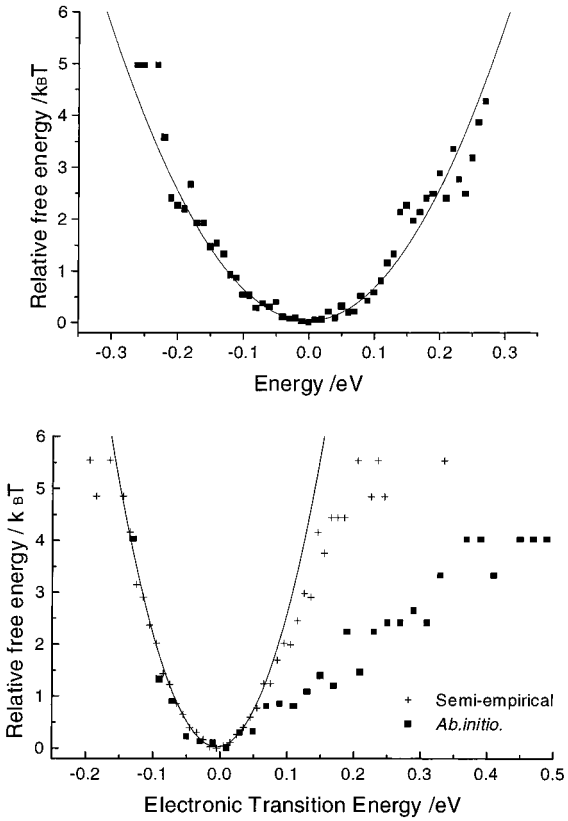

Figure 6. (a, top) Solvation energy (units of k_BT, $T = 298$ K) vs the electronic transition energy for BChl-a using the classical approach. Also shown is a quadratic curve (solid) fitted for free energies less than k_BT, and (b, bottom) solvation energy (units of k_BT) vs the electronic transition energy for BChl-a using the semiempirical approach (crosses) and ab initio approach (squares). Also shown is a quadratic curve (solid) fitted to the semiempirical results for a free energies less than k_BT.

tends to infinity i.e., an infinite bath. In the case shown in this work, the microscopic variable (the electronic transition energy) is determined not only by a broad range of poorly coupled frequencies but also by strongly coupled discrete frequencies. Take for example the limit of a single sinusoidal mode coupled to the electronic transition energy. For this case, the distribution of energy gap values will not tend to a Gaussian, even for sampling times that are arbitrarily large. Therefore, where the energy gap values are strongly influenced by a finite number of discretely coupled frequencies, the central limit theorem does not necessarily apply.

The side bands of the optical spectra (at approximately 700 nm for absorption and 875 nm for emission) are poorly represented in all of the calculations. There are a number of possible explanations for this. First, classical calculations of the vibrational dynamics are likely to represent modes much more accurately when they are in the high-temperature limit, i.e., modes of low frequency which are necessarily associated with a high quantum population at room temperature. In particular, we note here that the root mean squared deviations of classical and quantum oscillators are in general not identical. Second, we have shown that the contribution of different modes depends on the method of calculation that is used. Although the low-level *ab initio* approach works very well for the majority of significant modes, it may be that a higher level calculation is required to properly represent those modes which are responsible for the vibrational sideband. Third, the fluctuations for the *ab initio* approach deviate significantly from Gaussian, and it is possible that for this case, the cumulant expansion technique applied for the calculations of the optical response function is invalid. Fourth, although the main vibrational sideband occurs at an energy shift from the electronic origin which is approximately half the frequency of the OH and CH stretches, there is a chance that the use of SHAKE has influenced the sideband amplitudes somewhat. Finally, there is the possibility that the molecular mechanical component of the calculations is inadequate due to the charge fitting procedure which is used to establish the driving forces for the simulation, or indeed that the terms in the AMBER force field 32 are not adequate.

V. Conclusion

We have shown that an *ab initio* QM/MM method is capable of reproducing the experimental optical absorption and emission spectra for Bacteriochlorophyll-a in methanol. The Stokes shift, and therefore the reorganization energy, are well reproduced using either a semiempirical or ab initio method for calculation of the energy gap between the ground state and the first excited state. The fidelity with which the spectra are reproduced is rather sensitive to the method that is used.

We find that the *ab initio* calculations reproduce the spectra more accurately than the semiempirical calculations, with the *ab initio* method reproducing to some extent the Franck−Condon progression observed. The methods that involve a quantum calculation of the energy gap reproduce the spectra considerably better than the classical alternative. The quantum methods also predict rapid loss of memory, as shown by the autocorrelation function of the energy gap decaying rapidly with a half height width of 2−3 fs. The *ab initio* method has a contribution from underdamped high-frequency vibrations that are essential for close agreement with the experimental optical absorption profile. The overall effect is to produce a non-Gaussian distribution of solvation energies, and a free energy surface that departs significantly from quadratic for energies as low as k_BT.

Acknowledgment. I.R.G. acknowledges computational support from the EPSRC (GR/K 83878). We thank S. Abend for the measurements of the BChl-a spectra and A. Albrecht for a critical reading of the manuscript and helpful comments. D.R.K. and I.R.G. acknowledge support from the EPSRC.

References and Notes

(1) Carter, E. A.; Hynes, J. T. *J. Chem. Phys.* **1991**, *94*, 5961.
(2) Muino, P. L.; Callis, P. R. *J. Chem. Phys.* **1994**, *100*, 4093.
(3) Kumar, P. V.; Maroncelli, M. *J. Chem. Phys.* **1995**, *103*, 3038.
(4) Fleming, G. R.; Cho, M. *Annu. Rev. Chem.* **1996**, *47*, 109.
(5) Jimenez, R.; Fleming, G. R.; Kumar, P. V.; Maroncelli, M. *Nature* **1994**, *369*, 471.
(6) Mukamel, S. *Principles of Nonlinear Optical Spectroscopy*; Oxford University Press: London, 1995.
(7) Fonseca, T.; Ladanyi, B. M. *J. Phys. Chem.* **1991**, *95*, 2116.
(8) Brown, R. J. *Chem. Phys.* **1995**, *102*, 9059.
(9) Ando, K. J. *Chem. Phys.* **1997**, *107*, 4585.
(10) Maroncelli, M. *J. Chem. Phys.* **1990**, *94*, 2084.
(11) Maroncelli, M.; Fleming, G. R. *J. Chem. Phys.* **1988**, *89*, 5044.
(12) Levy, R. M.; Kitchen, D. B.; Blair, J. T.; Jespersen, K. K. *J. Phys. Chem.* **1990**, *94*, 4470.
(13) Bursulaya, B. D.; Zichi, D. A.; Kim, H. J. *J. Phys. Chem.* **1995**, *99*, 10069.
(14) Stratt, R. M.; Cho, M. *J. Chem. Phys.* **1994**, *100*, 6700.
(15) Fried, L. E.; Bernstein, N.; Mukamel, S. *Phys. Rev. Lett.* **1991**, *68*, 1842.
(16) Bruehl, M.; Hynes, J. T. *J. Phys. Chem.* **1992**, *96*, 4068.
(17) Rossky, P. J.; Simon, J. D. *Nature* **1994**, *370*, 263.
(18) Passino, S. A.; Nagasawa, Y.; Joo, T.; Fleming, G. R. *J. Phys. Chem.* **1997**, *101*, 725.
(19) de Boeij, W. P.; Pshenichnikov, M. S.; Wiersma, D. A. *J. Phys. Chem.* **1996**, *100*, 11806.

(20) Chandler, D. *Introduction of Modern Statistical Mechanics*; Oxford University Press: London, 1987.
(21) Ando, K.; Kato, S. *J. Chem. Phys.* **1991**, *95*, 5966.
(22) Hayashi, S.; Ando, K.; Kato, S. *J. Phys. Chem.* **1995**, *99*, 955.
(23) Carter, E. A.; Hynes, J. T. *J. Phys. Chem.* **1989**, *93*, 2184.
(24) Kubo, R. *J. Phys. Soc. Jpn.* **1962**, *17*, 1100.
(25) Kubo, R. *Adv. Chem. Phys.* **1969**, *15*, 101.
(26) Kubo, R. *Rep. Prog. Phys.* **1996**, *29*, 255.
(27) Mukamel, S. *J. Phys. Chem.* **1985**, *89*, 1077.
(28) Khidekel, V.; Chernyak, V.; Mukamel, S. *J. Chem. Phys.* **1996**, *105*, 8543.
(29) Ermler, U.; Fritzsch, G.; Buchanan, S. K.; Michel, H. *Structure* **1994**, *10*, 925.
(30) Stewart, J. J. P. *J. Comput. Chem.* **1989**, *10*, 209, 221.
(31) Stewart, J. J. P. MOPAC 93.00, Fujitsu Limited, Tokyo, Japan, 1993.
(32) Cornell, W. D.; Cieplak, P.; Bayly, C. I.; Gould, I. R.; Merz, K. M.; Ferguson, D. M.; Spellmeyer, D. C.; Fox, T.; Caldwell, J. W.; Kollman, P. A. *J. Am. Chem. Soc.* **1995**, *117*, 5179.
(33) Frisch, M. J.; Trucks, G. W.; Schlegel, H. B.; Gill, P. M. W.; Johnson, B. G.; Robb, M. A.; Cheeseman, J. R.; Keith, T.;. Petersson, G. A.; Montgomery, J. A.; Raghavachari, K.; Al-Laham, M. A.; Zakrzewski V. G.; Ortiz, J. V.; Foresman, J. B.; Cioslowski, J.; Stefanov, B. B.; Nanayakkara, A.; Challacombe, M.; Peng, C. Y.; Ayala, P. Y.; Chen, W.; Wong, M. W.; Andres, J. L.; Replogle E. S.; Gomperts, R.; Martin, R. L.; Fox, D. J.; Binkley, J. S.; Defrees, D. J.; Baker, J.; Stewart, J. P.; Head-Gordon, M.; Gonzalez, C.; J. A. Pople, *Gaussian 94, Revision D.3*; Gaussian Inc.: Pittsburgh, PA, 1995.
(34) Herhe, W. J.; Stewart, R. F.; Pople, J. A. *J. Chem. Phys.* **1969**, *51*, 2657.
(35) Binkley, J. S.; Pople, J. A.; Herhe, W. J. *J. Am. Chem. Soc.* **1980**, *102*, 939.
(36) Ditchfield, R.; Herhe, W. J.; Pople, J. A. *J. Chem. Phys.* **1971**, *54*, 724.
(37) Bayly, C. I.; Cieplak, P.; Cornell, W. D.; Kollman, P. A. *J. Phys. Chem.* **1993**, *97*, 10269.
(38) Pearlman, D. A.; Case, D. A.; Caldwell, J. W.; Ross, W. S.; Cheatham, T. E.; Ferguson, D. M.; Seibel, G. L.; Singh, U. C.; Weiner, P. K.; Kollman, P. A. AMBER 4.1, University of California, San Francisco, 1995.
(39) Caldwell, J. W., personal communication
(40) Van Gunsteren, W. F.; Karplus, M. *Macromolecules* **1982**, *15*, 1528.
(41) Van Gunsteren, W. F.; Berendsen, H. J. C. *Mol. Phys.* **1977**, *34*, 1311.
(42) Berendsen, H. J. C.; Postma, J. P. M.; Van Gunsteren, W. F.; DiNola, A.; Haak, J. R. *J. Chem. Phys.* **1984**, *81*, 3684.